High-power near diffraction-limited 1 064-nm Nd:YAG rod laser and second harmonic generation by intracavity-frequency-doubling

Shubao Zhang (张树宝)[1,2], Lin Guo (郭 林)[1], Menglong Li (李梦龙)[1,2], Ling Zhang (张 玲)[1], Xin Yan (鄢 歆)[1], Wei Hou (侯 玮)[1], Xuechun Lin (林学春)[1*], and Jinmin Li (李晋闽)[1]

[1] *Laboratory of All-Solid-State Light Sources, Institute of Semiconductors, Chinese Academy of Sciences, Beijing 100083, China*

[2] *Graduate University of Chinese Academy of Sciences, Beijing 100049, China*

[*] *Corresponding author: xclin@semi.ac.cn*

Received September 22, 2011; accepted December 12, 2011; posted online March 28, 2012

We present a near diffraction-limited 1 064-nm Nd:YAG rod laser with output power of 82.3 W (M^2 ≈1.38). The power fluctuation over two hours is better than ±1.1%. Pulsed 1 064-nm laser with an average power of 66.6 W and pulse width of 46 ns are achieved when the laser is Q-switched at a repetition rate of 10 kHz. The short pulse duration stems from the short cavity as well as the high-gain laser modules. Using intracavity-frequency-doubling, a 35.0-W near diffraction-limited 532-nm green laser (M^2 ≈1.32) is achieved with a pulse width of 43 ns.

OCIS codes: 140.0140, 140.3580, 140.3410, 140.3515.
doi: 10.3788/COL201210.071401.

Due to their varied applications, high-power green lasers with side-pumped Nd:YAG rod lasers have developed rapidly in the last decade[1−9]. The output power of the green laser exceeds 400 W[7]. However, the reported green lasers[1−9] suffer from low beam quality (M^2 >10), because the side-pumped Nd:YAG rod is influenced by severe thermal effects, such as thermal lensing and thermal birefringence. Moreover, it is very difficult to achieve a good match between the TEM_{00} mode and the pumping volume. Few studies have reported high-power green lasers with high beam quality and side-pumped Nd:YAG modules, which are usually obtained by extracavity-frequency-doubling with a complex end-pumped master-oscillator power amplifier (MOPA) system[10−12] or a complex injection seeded system[13]. However, Hirano *et al.* have reported an output power of 208-W TEM_{00} 1 064-nm laser with two specially designed side-pumped Nd:YAG modules[14], which has the potential to obtain high-power high-beam-quality second harmonic generation (SHG) with a compact intracavity-frequency-doubling system.

In this letter, we report a high-power high-beam-quality 1 064-nm Nd:YAG rod laser and SHG by intracavity-frequency-doubling. We used a short symmetrical cavity with two concave mirrors compensating for the thermal focal effect of the Nd:YAG rod. Compared with the complex end-pumped MOPA or injection seeded system, the symmetric cavity is compact and can easily achieve a hundred-watt level near the diffraction-limited laser beam. Moreover, in comparison with the conventional unstable resonators, the plane-parallel cavity has a wider thermal stability region according to the theoretical calculation with the standard ABCD ray propagation matrix. The configuration of the cavity is demonstrated to have a good scheme for high-power TEM_{00} 1 064-nm laser generation[14]. With two common side-pumped Nd:YAG rod modules in the short cavity, we achieved an 82.3 W near diffraction-limited continuous wave (CW) 1 064-nm laser (M^2 ≈1.38) with a good power stability of ±1.1% for over two hours. The output power and pulse duration with different Q-switched frequencies of 10, 15, and 20 kHz are also studied. A pulsed 1 064-nm laser beam with pulse width of 46 ns is achieved at a Q-switched frequency of 10 kHz and an average output power of 66.6 W. Finally, a 35.2-W pulsed green laser with a pulse width of 43 ns in a near diffraction-limited beam (M^2 ≈1.32) is generated using an LBO crystal as the frequency doubler in the cavity.

The schematic diagram of the resonator is shown in Fig. 1. Two common side-pumped Nd:YAG laser modules were selected in the experiment. In the laser head, the Nd:YAG rod (3 mm in diameter and 65 mm in length, with 0.8 at.-% Nd doping) was side-pumped using 9 diode bars in a 3-fold symmetry with an available maximum pump power of approximately 270 W at CW 808 nm when working at a drive current of 30 A. The Nd:YAG

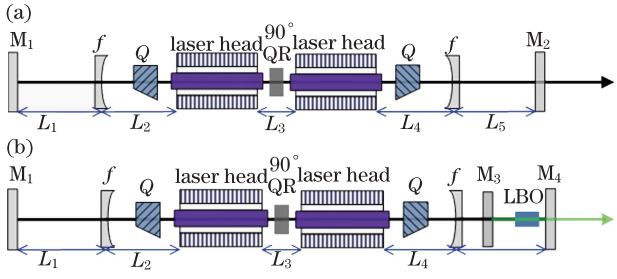

Fig. 1. Schematic diagrams of (a) IR experiment and (b) SHG experiment. Laser head: diode-side-pumped laser module; Q: acousto-optic Q-switch; QR: quartz rotator; M_1: plane total reflector; M_2: plane partial reflector R=50%; M_3 and M_4: plane dichroic mirrors; f: plane-concave lens f=−100 mm.

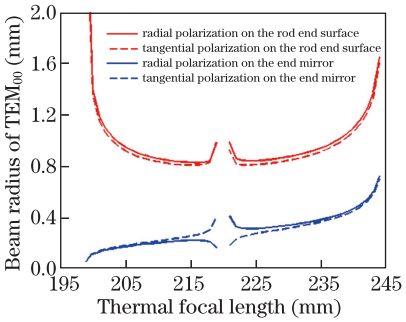

Fig. 2. Beam radii of TEM_{00} mode on the end surface of the Nd:YAG rod and the end mirror M_2 versus the average thermal focal length. Solid line represents radial polarization, and the dashed line represents tangential polarization.

rod and the diode bars were cooled with flowing water, and the temperature of the cooling water was maintained at 20 °C(±0.1 °C).

The conventional and effectual configurations—two identical laser heads with a 90° quartz polarization rotator between them—were used for compensating the polarization-dependent thermally-induced birefringence. The laser heads were placed close to each other, so that the beam radius between them remained uniform. In the experiment, the distance between the laser heads L_3 was fixed at about 35 mm. The effective thermal-induced birefringence compensation ensured that the beam radius of the radial polarized and the tangential polarized component were nearly the same at the same average thermal focal length[9]. In order to improve the hold-off capacity, we employed two acousto-optic (AO) Q-switches (QSG40-1Z, CETC) which were placed orthogonally alongside the laser heads and driven synchronously by a single power supply. Moreover, the two Q-switches assured the symmetry of the resonator, as well.

In order to realize stable TEM_{00} mode oscillation, a large TEM_{00} mode size is required to suppress the high-order mode[15,16]. Two plane-concave lenses with the same focal length of –100 mm were utilized to enlarge the beam radius of the TEM_{00} mode. Using the standard ABCD ray propagation matrix with different cavity parameters, we calculated the beam radius of the TEM_{00} mode on the end surface of the Nd:YAG rod and the end mirror M_2 versus the average thermal focal length. The pumped Nd:YAG rod was treated as a lens-like medium, and the ray transfer matrix was introduced in Ref. [17], along with the relationships of the radial focal length f_r, the tangential focal length f_φ, and the average thermal focal length f. Considering both the overlap efficiency and the diffraction effects at the rod aperture, the minimum beam radius ω_0 in the end surface of the rod was designed to be about 0.8 mm. The cavity parameters were then optimized according to the output power at 1 064 nm and finally chosen to be L_1=L_5=120 mm and L_2=L_4=145 mm with a cavity length of about 700 mm. The calculated beam radius of TEM_{00} mode versus the thermal focal length is shown in Fig. 2. There is a narrow unstable region around the average thermal length f=220 mm. The beam sizes of the two polarized components were nearly the same, with the minimum beam radius ω_0 ≈0.8 mm. The unstable region is caused by the asymmetry brought about by the single polarization component; this is because during one cycle in the resonance, it undergoes the radial focal length f_r (the tangential focal length f_φ) in one laser head and the tangential focal length f_φ (the radial focal length f_r) in the other after the 90° quartz rotator.

As for the SHG, a type II phase-matched LBO crystal (4×4×18 mm^3, θ=27.2°, φ=90.0°) was selected as the frequency-doubler for its high damage threshold and nonlinear coefficient[11,18]. The LBO crystal was AR coated at 532 and 1 064 nm (T >99.8% @1 064 nm and T >99.5% @532 nm) at the end surfaces. Due to the sensitivity of the SHG output to LBO temperature, a copper oven with a precision of ±0.1 °C was used to mount the LBO crystal. The oven was placed as close to the end dichroic mirror M_4 (0° R >99.8% @1 064 nm & T >98.5% @532 nm) as possible (Fig. 1 (b)), where the laser spot size was small. This was done in order to obtain high power density in the LBO crystal. After the total reflection of the dichroic mirror M_3 (0° T >99.8% @1 064 nm and R >99.5% @ 532 nm), the 532-nm green laser, generated in two directions, was extracted unidirectionally from the dichroic mirror M_4.

The output power at 1 064 nm versus the optical pump power with an optimum partial reflector (R=50% at 1 064 nm) is shown in Fig. 3. A maximum output power of 82.3 W at CW 1 064 nm is achieved when the optical pump power increased to about 432 W. The corresponding optical-to-optical and electrical-to-optical efficiencies are 19.5% and 7.9%, respectively. The beam quality factor M^2 at the output power of 82.3 W is measured to be 1.38 by parabolic fitting[2] (Fig. 4). The beam radii at different positions after focusing using a lens (f=200 mm) were measured with a laser beam analyzer

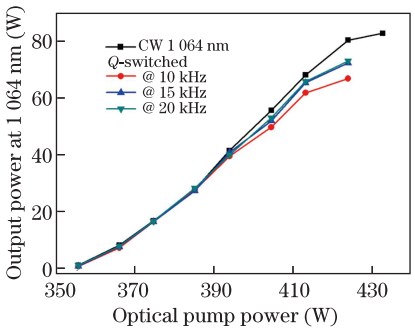

Fig. 3. Output power of 1 064-nm laser versus the optical pump power.

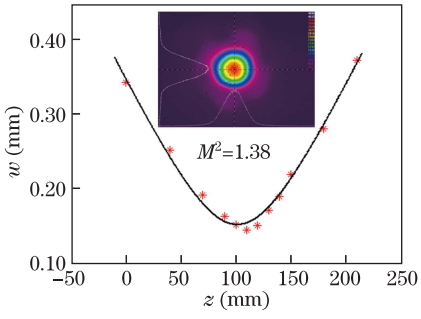

Fig. 4. M^2 measurement of CW 1 064-nm laser at about 82 W. Inset is the typical two-dimensional beam profiles by Spiricon LBA-FW-SCOR.

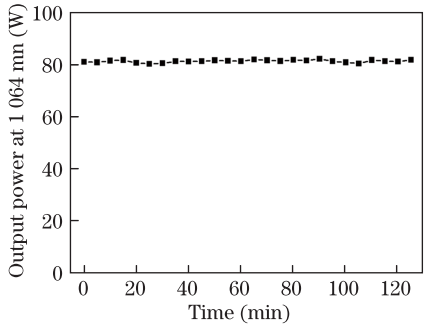

Fig. 5. Power fluctuations of CW 1 064-nm laser at about 82 W.

(Spiricon Inc.) After studying the output power stability of CW 1 064-nm laser beam by recording the instantaneous value of the power meter every 5 mins, we find that the power fluctuation for over 2 hours is better than ±1.1% (Fig. 5).

When operating at the Q-switched mode, the maximum available pump power decreases to about 423 W because of increased heat generation during the no lasing intervals. Figure 6 shows the average output power and pulse width at 1 064 nm versus the pulse repetition frequency. When Q-switched at a repetition rate of 10 kHz, an average power of 66.6 W is obtained with pulse width of 46 ns, corresponding to a peak power of about 144.8 kW. Compared with our previous experiment[9], the short pulse duration in the present work stems from the short cavity as well as the high-gain laser modules. As the Q-switching frequency increases to 15 kHz, the average power also increased to 71.9 W with an amplitude of 5.3 W; the pulse width also increased to 55 ns, resulting in a decreased peak power of 87.2 kW. When the Q-switching frequency increases to 20 kHz, a maximum average power of 72.6 W is obtained with an increase of less than 1 W. However, as the pulse width increases to 68 ns, the peak power drops to 53.4 kW. Given that the efficiency of SHG is directly proportional to the power density of the fundamental beam[19], a higher efficiency is expected with Q-switching at a lower repetition frequency. This has been demonstrated in the latter experiment.

We replaced the output coupler M_2 with the dichroic mirror M_4, set the oven with the LBO crystal as close to mirror M_4 as possible, and inserted the dichroic mirror M_3 into the cavity (Fig. 1 (b)). SHG by intracavity-frequency-doubling was carried out under different Q-switching frequencies of 10 and 15 kHz. LBO temperature was optimized every time the pump power was increased to obtain the optimal SHG. The average output power at 532 nm is shown in Fig. 7. Under the Q-switching frequency of 10 kHz, an average output power of 35.0 W at 532 nm (M^2 ≈1.32, Fig. 8) is generated with pulse width of 43 ns. However, the maximum output power decreases to 29.5 W when the Q-switches operate at 15 kHz; in addition, the decrease of the output power at 532 nm results from the decline of the peak power of the fundamental beam as the pulse repetition rate increases. In fact, the diachronic mirror M_3 could be removed if the plane surface of the right lens (Fig. 1(b)) is AR coated at 1 064 nm and HR coated at 532 nm (0° T >99.8% @1 064 nm and R >99.5% @ 532 nm). It is expected that a higher output power at 532 nm would be achieved due to less insert loss.

In conclusion, we report a high-power near diffraction-limited 1 064-nm laser with two common side-pumped Nd:YAG rod modules in a symmetry cavity. Two plane-concave lenses (f=–100 mm) are inserted into the cavity to enlarge the TEM_{00} beam radius on the end surface of Nd:YAG rod (ω_0 ≈0.8 mm). With this configuration, we obtain an output power of 82.3 W at CW 1 064 nm in a near diffraction-limited beam (M^2 ≈1.38) with good power stability of ±1.1% for over 2 hours. The corresponding optical-to-optical and electrical-to-optical efficiencies are 19.5% and 7.9%, respectively. The low optical-to-optical efficiencies of side-pumped Nd:YAG lasers operating in near diffraction-limited mode increase the generation of heat and limit the power scaling of the near diffraction-limited laser beam. The output power and pulse duration with different Q-switched frequencies of 10, 15, and 20 kHz are studied in the present work. When Q-switched

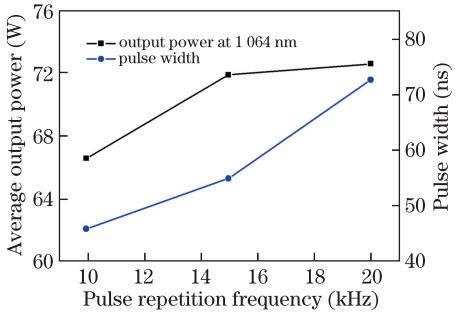

Fig. 6. Average power and pulse width of 1 064-nm laser versus pulse repetition frequency.

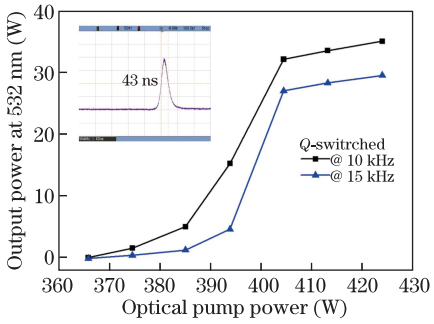

Fig. 7. Average output power of 532-nm green laser versus the optical pump power.

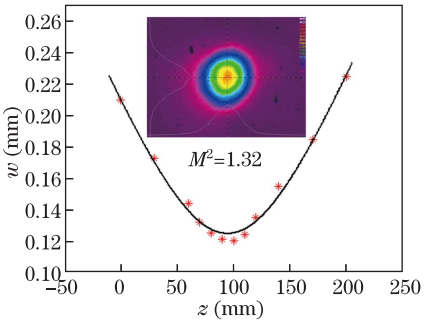

Fig. 8. M^2 measurement of 532-nm green laser at about 35 W. Inset is the typical two-dimensional beam profiles by Spiricon LBA-FW-SCOR.

at a repetition rate of 10 kHz, an average power of 66.6 W at 1 064 nm is achieved, with pulse width of 46 ns and a peak power of 144.8 kW. Through intracavity-frequency-doubling with an LBO crystal, we obtained 35.0 W near diffraction-limited 532-nm green laser (M^2 ≈1.32) with a pulse repetition rate of 10 kHz; in addition, the pulse width of the green laser is 43 ns. The average power of the green laser decreases to 29.5 W when the Q-switches operate at 15 kHz. The decrease of the second harmonic power is mainly caused by the decline of the peak power; this is because the power density of the fundamental wave is a crucial factor in SHG.

This work was supported by the National Key Scientific Research Project of China (No. 2012CB934200), the National "863" Program of China (No. 2011AA030206), and the Knowledge Innovation Program of the Chinese Academy of Sciences (No. KGCX2-YW-399+10).

References

1. J. J. Chany, E. P. Dragon, C. A. Ebbers, I. L. Bass, and C. W. Cochran, Advanced Solid State Lasers **19,** 300 (1998).
2. S. Konno, T. Kojima, S. Fujikawa, and K. Yasui, Opt. Lett. **25,** 105 (2000).
3. J. Yi, H.-J. Moon, and J. Lee, Appl. Opt. **43,** 3732 (2004).
4. D.-G. Xu, J.-Q. Yao, B.-G. Zhang, R. Zhou, E. Li, S.-Y. Zhao, X. Ding, W.-Q. Wen, Y.-X. Niu, J.-G. Hu, and P. Wang, Opt. Commun. **245,** 341 (2005).
5. A. Geng, Y. Bo, Y. Bi, Z. Sun, X. Yang, Q. Peng, H. Li, R.Li, D. Cui, and Z. Xu, Opt. Lasers in Eng. **44,** 589 (2006).
6. Y. Bo, Q. Cui, A. Geng, X. Yang, Q. Peng, Y. Lu, D. Cui, and Z. Xu, in *Proceedings of Conference on Lasers and Electro-Optics* CTuD4 (2007).
7. D. R. Dudley, O. Mehl, G. Y. Wang, E. S. Allee, H. Y. Pang, and N. Hodgson, Proc. SPIE **7193,** 71930Z (2009)
8. Sh. B. Zhang, Q. J. Cui, B. Xiong, L. Guo, W. Hou, X. C. Lin, and J. M. Li, Laser Phys. Lett. **7,** 707 (2010).
9. S. Zhang, L. Guo, B. Xiong, Y. Liu, W. Hou, X. Lin, and J. Li, Appl. Phys. B **104,** 861 (2011).
10. T. Riesbeck and H. J. Eichler, Opt. Commun. **275,** 429 (2007)
11. Q. Liu, X. Yan, M. Gong, X. Fu, and D. Wang, Opt. Express **16,** 14335 (2008)
12. K.-H. Hong, C.-J. Lai, A. Siddiqui, and F. X. Kärtner, Opt. Express **17,** 16911 (2009)
13. J. Wang, R. Zhu, J. Zhou, H. Zang, X. Zhu, and W. Chen, Chin. Opt. Lett. **9,** 081405 (2011).
14. Y. Hirano, Y. Koyata, S. Yamamoto, K. Kasahara, and T. Tajime, Opt. Lett. **24,** 679 (1999).
15. G. Cerullo, S. D. Silvestri, V. Magni, and O. Svelto, Opt. Quantum Electron. **25,** 489 (1993).
16. M. P. Murdough and C. A. Denman, Appl. Opt. **35,** 5925 (1996).
17. S. Lee, M. Yun, B. H. Cha, C. J. Kim, S. Suk, and H. S. Kim, Appl. Opt. **41,** 5625 (2002).
18. S. Lin, Z. Sun, B. Wu, and C. Chen, J. Appl. Phys. **67,** 634 (1990).
19. W. Koechner, *Solid-State Laser Engineering* (6th ed.) (Springer, Berlin, 2006).